Journal of Biotechnology 387 (2024) 32–43

Contents lists available at ScienceDirect

Journal of Biotechnology

journal homepage: www.elsevier.com/locate/jbiotec

Practical deployment of automation to expedite aqueous two-phase extraction

Mario A. Torres-Acosta [a,b], Alex Olivares-Molina [a], Ross Kent [c], Nuno Leitão [c], Markus Gershater [c], Brenda Parker [a], Gary J. Lye [a], Duygu Dikicioglu [a,*]

[a] The Advanced Centre for Biochemical Engineering, Department of Biochemical Engineering, University College London, London WC1E 6BT, United Kingdom
[b] Tecnologico de Monterrey, School of Engineering and Science, Av. Eugenio Garza Sada 2501 Sur, Monterrey, N.L. 64849, México
[c] Synthace Ltd., The Westworks 4th Floor, 195 Wood Lane, W12 7FQ, United Kingdom

ARTICLE INFO

Keywords:
Aqueous two-phase extraction
Liquid handling device
Automation
Optimisation
Phase diagrams
Binodal curve
Process development

ABSTRACT

The feasibility of bioprocess development relies heavily on the successful application of primary recovery and purification techniques. Aqueous two-phase extraction (ATPE) disrupts the definition of "unit operation" by serving as an integrative and intensive technique that combines different objectives such as the removal of biomass and integrated recovery and purification of the product of interest. The relative simplicity of processing large samples renders this technique an attractive alternative for industrial bioprocessing applications. However, process development is hindered by the lack of easily predictable partition behaviours, the elucidation of which necessitates a large number of experiments to be conducted. Liquid handling devices can assist to address this problem; however, they are configured to operate using low viscosity fluids such as water and water-based solutions as opposed to highly viscous polymeric solutions, which are typically required in ATPE. In this work, an automated high throughput ATPE process development framework is presented by constructing phase diagrams and identifying the binodal curves for PEG6000, PEG3000, and PEG2000. Models were built to determine viscosity- and volume-independent transfer parameters. The framework provided an appropriate strategy to develop a very precise and accurate operation by exploiting the relationship between different liquid transfer parameters and process error. Process accuracy, measured by mean absolute error, and device precision, evaluated by the coefficient of variation, were both shown to be affected by the mechanical properties, particularly viscosity, of the fluids employed. For PEG6000, the mean absolute error improved by six-fold (from 4.82% to 0.75%) and the coefficient of variation improved by three-fold (from 0.027 to 0.008) upon optimisation of the liquid transfer parameters accounting for the viscosity effect on the PEG-salt buffer utilising ATPE operations. As demonstrated here, automated liquid handling devices can serve to streamline process development for APTE enabling wide adoption of this technique in large scale bioprocess applications.

1. Introduction

The development of biological products for manufacturing at scale is heavily reliant on the availability of appropriate primary recovery and purification techniques (Tripathi and Shrivastava, 2019). These can be collectively referred to as downstream bioprocessing methods. Depending on the intended use, various unit operations can be combined to achieve the desired level of purity and product quality (Tripathi and Shrivastava, 2019). The required product specifications to be met as well as the complexity of the process to meet these specifications can render downstream processing very costly to operate. This challenge raises the question about how unit operations should be viewed and optimised as bioprocessing sector advances.

Automation has developed into an outstanding tool for obtaining results quickly while minimising the commitment a researcher must make with respect to available resources (Torres-Acosta et al., 2022). Liquid handling devices (LHD), in particular, made it possible to automate the manipulation of liquids. Furthermore, it's been noted that a variety of conventional experiments or some of their aspects can be condensed and separated into simple tasks (Groth and Cox, 2017) such as pipetting, dilution, mixing, and aliquoting. This has substantially increased the usage of LHD in a range of applications. Even more

* Corresponding author.
E-mail address: d.dikicioglu@ucl.ac.uk (D. Dikicioglu).

https://doi.org/10.1016/j.jbiotec.2024.03.013
Received 25 January 2024; Received in revised form 15 March 2024; Accepted 26 March 2024
Available online 28 March 2024

importantly, the recent Covid-19 pandemic has shown that these tools should be an essential component of any laboratory (Taylor et al., 2021; Cortez et al., 2022; Villanueva-Cañas et al., 2021; Crone et al., 2020; Paton et al., 2021; Basu et al., 2021). It was shown that LHD were capable of processing a large number of samples quickly and gently, with the ability to work at even nanolitre scales. In bioprocessing, the incorporation of LHD into downstream process development provided invaluable data on protein purification by adapting chromatographic analysis into small scale columns operating in parallel (Cibelli et al., 2022; Kiesewetter et al., 2016).

However, due to process complexity and the necessity for meticulous LHD adaptation, process development and optimisation concerning many bioprocessing operations have not yet fully embraced automation. Liquid-liquid extraction is a unit operation that, in theory, should be simple to implement in an LHD since it is purely reliant on the use of liquids (Iqbal et al., 2016). Aqueous two-phase extraction (ATPE), which is a method that often relies on the availability of biocompatible elements over a critical concentration to promote the formation of two phases, offers a powerful alternative for the purification and separation of biological products, such as proteins, allowing the product and the contaminants to partition into different phases (Iqbal et al., 2016). As such, pharmaceutical grade purification was achieved by ATPE for certain substances, such as enzymes and antibodies, and the operation could be scaled up with relative ease (Mao et al., 2010; Schmidt et al., 2017; Kruse et al., 2020; Rosa et al., 2009).

The absence of a suitable prediction platform that can estimate partition behaviours is currently one of the main barriers hindering the widespread deployment of ATPE in industrial operations (Torres-Acosta et al., 2019). The requirement to conduct many experimental runs in order to construct phase diagrams, their corresponding binodal curves, and subsequent product purification profile only adds to these challenges. It has been suggested that automation of ATPE processes could reduce this burden by increasing sample size, creating more complex high throughput screening configurations, and utilising various optimization strategies (Bussamra et al., 2019).

It is customary to create phase diagrams for early stage ATPE process development. These diagrams show the relative quantities of the various phase-forming compounds, as well as denoting the boundary between the one- and two-phase solutions, i.e., the binodal curve. The binodal curve is subsequently used as reference to determine the composition of the solution and to evaluate the partitioning behaviour in future experiments. The volume ratio (V_R) between the top and bottom phases is indicated by the tie lines, which also show the mass composition of each phase. Data of increasing size can be gathered and plotted to produce tie lines as characterized by their length within the plot.

Phase diagrams and binodal curves can be obtained in a variety of ways (Kojima et al., 2019; Silva et al., 2014). The cloud point approach, which is based on visual changes as a solution is titrated with another that may eventually form a second phase, is the most widely used technique (Fakhari and Rahimpour, 2020). This is labour intensive, and it relies on qualitative techniques. In some cases, the approximate proportions needed to create a two-phase mixture are known, and that specific region of the phase diagram is the focus of attention. In other cases, this is not known, rendering it vital to explore the whole range of solutions that account for a variety of potential outcomes. These methods can be employed in combination to achieve the desired outcome in the most efficient way.

Mixtures based on polymers such as polyethylene glycol (PEG) or dextran and salts such as phosphates or sulphates are among the most extensively studied ATPE mixtures (Iqbal et al., 2016). The high viscosity of the polymer solutions in these mixtures renders both manual and automated operation difficult (Rahbari-Sisakht et al., 2003). The final volume of fluid that is transferred could potentially vary depending on the velocity at which it is aspirated or dispensed depending on its viscosity (Soh et al., 2023). Additionally, when pipetting tips are immersed in viscous liquid, a liquid film forms on the exterior, causing the tips to drag more liquid than intended. This final challenge also introduces problems of contamination of the devices used in analysis. For this reason, it is imperative to understand the impact that every possible viscous polymer (e.g. PEG) - salt mixture composition has on the performance of a liquid handling device and develop a strategy to mitigate potential errors.

This work presents the first framework for automated construction of phase diagrams for two-phase mixtures, which overcomes the challenges highlighted above. In this pipeline, the suitable liquid handling parameters are determined for a system of broad interest in order to advise and assist future experiments. Here, phase diagrams and associated binodal curves were constructed for a range of compositions using PEG (2000, 3000, and 6000) – KH_2PO_4/K_2HPO_4 (namely phosphate buffer) mixtures as benchmarks. The binodal curves were then used to compare the process performance when optimised and non-optimised transfer parameters were employed in the operation of the LHD. This work is the first of its kind on performing a comprehensive analysis on the impact of the liquid to be manipulated on the liquid handling parameters required for its transfer and the swiftest phase diagram generation strategy reported to date, which allows rapid determination of the binodal curves to expeditated ATPE.

2. Materials and methods

2.1. Equipment and chemicals

This procedure employed automated experimentation using a Tecan EVO 200 (Tecan Group Ltd.). The device consists of one Robotic Manipulator (RoMa) arm and one Liquid Handling arm (LiHa) with eight pipetting channels and disposable tips (DiTis). It utilises carbon coated DiTis to calculate the liquid level based on liquid conductivity. DiTi plate carriers, locations for troughs to hold liquid reservoirs, and a wash station are other components located on the device deck. Synthace platform was used to create automated protocols (Synthace Ltd., UK) to be used in the LHD. The platform uses experiment-like commands referred to as "Elements" to streamline the construction of workflows (see Supplementary Material for the specific workflows created for this work).

To test the transfer of a liquid by the LHD, the weight of solution transferred was determined utilising a weighing scale (Sartorius AG, Germany – model BL610) for manual manipulation of ATPE components and verification of mass transfer by the LHD. Consumables for the LHD included 100 mL throughs, 1 mL and 200 μL disposable tips (DiTi), all of which were acquired from Axygen (Corning, Inc., Mexico). Additionally, 2 mL 96 deep-well plates and UV-clear 96-well plates (Scientific Laboratory Supplies, UK) were used.

All chemicals were purchased from Millipore Sigma (Merck KGaA, Germany). PEG2000, PEG3000, and PEG6000 were prepared at 60 wt% concentration using Milli-Q water. A K_2HPO_4/KH_2PO_4 (6.3 M) buffer at pH 7.5 (from here on “the phosphate buffer”) was used to prepare the ATPE mixtures. The colouring agent Methyl Orange (MO), which partitions to the top phase in a PEG-salt system, was used to visualise phase formation (0.1 mM). Milli-Q water (Merck KGaA, Germany) was used for preparing the solutions. All experiments were performed at room temperature (23 °C).

2.2. Experimental methodology

ATPE curves are typically constructed using weight percentages, which means that for a system, for example, of 1 g total weight that contains 50 wt% PEG and 30 wt% phosphate buffer, this translates to 0.5 g of PEG and 0.3 g of phosphate buffer and 0.2 g of water. In this work, mixtures of PEG-salt-water were used to monitor the accurate movement of a viscous solution during automated transfer. After each liquid movement, the weight of the transferred solution was measured and compared to its expected value. Characterising the density and

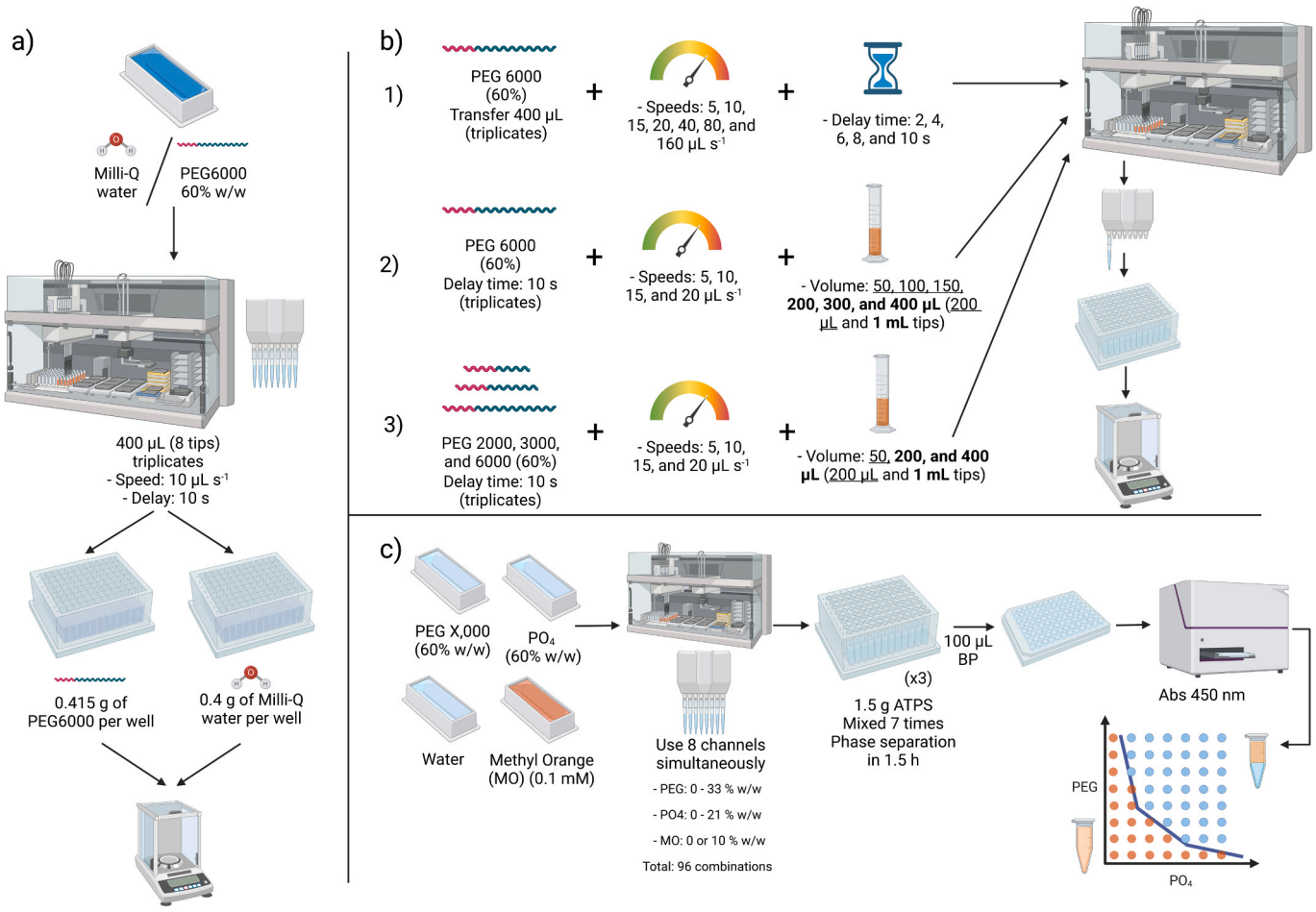

Fig. 1. Schematic representation of the experimental framework. Preliminary experiments were employed to determine the accuracy and the precision of the setup when transferring PEG6000 and water mixture (60 wt%) (a). The interplay between aspiration/dispense speed, delay time, volume to be transferred and PEG size (ergo, varying fluid viscosity) was investigated in order to determine the optimal liquid transfer parameters (b). The optimised parameters were then used to construct phase diagrams and to determine the corresponding binodal curves (c).

viscosity of water and the working solutions of PEG2000, PEG3000, and PEG6000 was a preliminary component of this set of experiments.

Since the transfer of viscous liquids presents a variety of challenges, it is crucial to establish the accuracy and the precision of the experiment. A number of serious problems arise when a viscous liquid is aspirated quickly. Air easily gets trapped in the pipetting tip and the mechanical part of the pipette may face the risk of contamination. The formation of fluid films when viscous liquids were mixed with a gas was investigated to demonstrate that the layers of liquid are stuck to the wall of their path (Czernek and Witczak, 2020). This explains the observed phenomenon of viscous liquids not adequately being removed from the tip of a pipette. Furthermore, the transfer of the liquid into or out of the tip is typically delayed when working with viscous liquids and solutions (Soh et al., 2023). Literature has shown how different aspiration and dispense speed programmed into a LHD are different to the actual transfer speed when employing a viscous liquid (Soh et al., 2023). Finally, the drag on the exterior of the pipetting tip may lead to spills into other labware or an excessive amount of fluid being transferred to the intended site. The behaviour of viscous liquid on a pipette has even been suggested as a platform to determine some rheologic properties (Wang et al., 2021). To analyse this behaviour, a 3-part experimental framework was developed (Fig. 1) where the LHD's accuracy and precision were tested first to address these challenges.

Establishing a correlation between various factors and the actual mass of material being transferred constituted the second part of the experiment. This exercise identified the specific movement parameters to ensure successful mass transfer in the LHD for the viscous polymer. Here, aspiration/dispense speed (speed) and delay time (delay time), volume to be transferred, and length of the polymer (PEG size) were taken into consideration as factors.

The final step of the methodology consisted of testing outputs from the first two steps of the framework. This involved constructing three phase diagrams, one for each of the PEG sizes that were tested here and determining their cognate binodal curves. A range of 96 mixture combinations were tested in order to explore the experimental space and identify the interface between the single-phase and two-phase mixtures. The number of mixtures tested was confined to the capacity of a single 96 deep-well plate in order to exclude any potential plate-to-plate variation that would factor into parameter testing.

2.2.1. *Evaluation of experimental accuracy and device precision*

ATPE curves are constructed using weight percentages; all liquid transfers were verified by the transferred mass, and this was done by weighing the liquids. The densities of all PEG stocks were determined manually. Then, 400 µL (0.415 g) of PEG6000 from a 60-weight percent (%wt) stock or 400 µL Milli-Q water (0.4 g) were transferred into a 96-deep well plate (with a maximum well capacity of 2 mL) using all 8 tips in the LiHa, and the transferred weights were recorded. This experiment was conducted in triplicates (Fig. 1a).

This experiment used a slow liquid transfer speed of 10 µL s^{-1} and an extended delay time of 10 s following aspiration/dispense to evaluate the viscous liquid dispensing performance of the LHD. Accuracy was

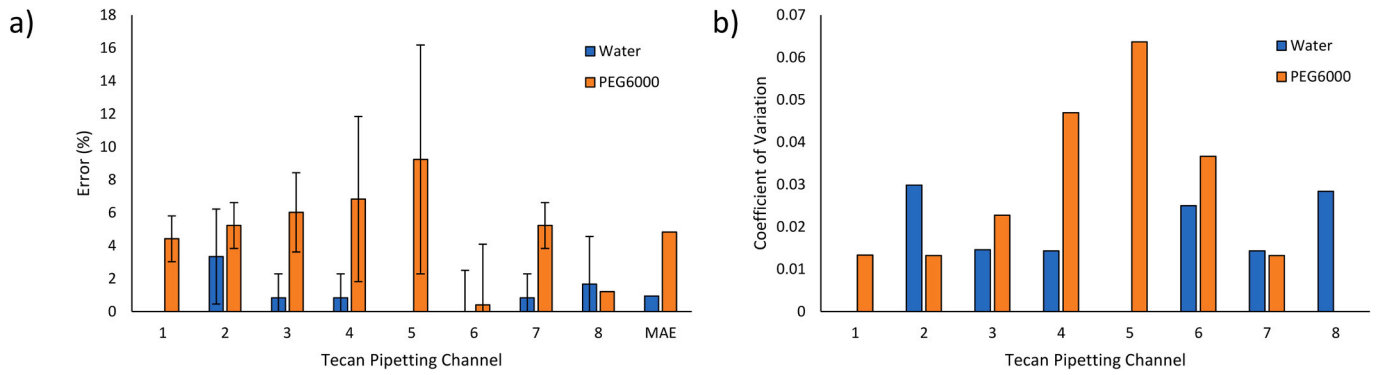

Fig. 2. Analysis of accuracy and precision. Accuracy was analysed by measuring the error percentage (%) and the Mean Absolute Error (MAE) (a), while precision was analysed by considering the coefficient of variation within each pipetting channel (b). Water and PEG6000 (60 wt%) were used since the liquid handling device (LHD) is originally configured to operate with water-like fluids, while PEG6000 presents a case evaluating the device performance for high viscosity solutions. Bars represent mean values, while error bars denote the standard deviation around the mean.

determined by quantifying the error percentage and the mean absolute error (MAE) (Eqs. 1 and 2, respectively) between the measured weight and the expected weight calculated from the volume input and the calculated density (Bessemans et al., 2016). The standard deviation (SD) between samples, shown as an error bar in Fig. 2a, and the coefficient of variation, which indicates the ratio of the standard deviation to the mean, were calculated to evaluate the precision (Czernek and Witczak, 2020).

$$Error \quad (\%) = \frac{Measured \quad Value - Expected \quad Value}{Expected \quad Value} \times 100\% \tag{1}$$

$$Mean \quad Absolute \quad Error \quad (MAE - \%) = \frac{\sum_{i=0}^{n} |Error|}{n}; i = Pipetting \quad channels \tag{2}$$

2.2.2. Correlation between technical parameters and experimental variables

Experiments were conducted in three stages to determine a correlation between the technical parameters: speed and delay time (terms as described above) and the experimental variables: volume to be transferred and the PEG size impacting fluid viscosity, against the transfer error in the LHD. The impact of speed and delay time on a fixed volume of fluid transfer (400 μL) at a fixed viscosity (PEG6000 stock at 60 wt%) was determined first. Viscosity values were determined using a rotational rheometer (Kinexus Prime, Netzsc, Germany) operating at a constant temperature of 25 °C until viscosity readings were stable. The explored speed range was 5–160 μL s^{-1} and the delay time was varied between 2 and 10 s in increments of 2 s. All eight pipetting tips in the LiHa were used simultaneously and the experiment was conducted in triplicates for each condition.

In the second stage, the delay time was fixed at the value of 10 s and the viscosity of the fluid was fixed (PEG6000 stock at 60 wt%), while the speed as well as the volume of fluid to be transferred were varied. The speed range to be tested was reduced (5–20 μL s^{-1}) and the volume to be transferred was varied in a range from 50 to 400 μL. To ensure liquid handling precision at low volumes, all volumes < 200 μL were transferred using a 0.2 mL DiTi, while the 1 mL DiTi were used for the remaining volumes.

The third stage of this process development studied the relationship between speed, volume to be transferred, and the PEG size. The speed and volume ranges evaluated were similar to those used in the second stage of this experiment, and the solution viscosity was varied by using PEG stocks with a molecular size of 2000, 3000, and 6000 at 60 wt% (Fig. 1b).

For all tested conditions, the weight after each liquid transfer was recorded and compared against the expected weight for error calculations. Linear regression models were constructed to correlate each variable against the error percentage. Appropriate speeds achieving a theoretical zero error percentage were determined via subsequent analysis of the linear regression models. Where appropriate, comparison between datasets was performed using ANOVA and Tukey post-hoc test (α = 0.01) (Microsoft Excel (Microsoft, USA) or SPSS version 25 (IBM Corp., USA)). The data from at least three replicate runs were compared for statistical analyses.

2.2.3. Construction of phase diagrams and binodal curves

Phase diagrams were constructed for the mixture of PEG (2000, 3000, and 6000) and the phosphate buffer to identify the binodal curve describing the separation characteristics of these mixtures. For this identification different ranges of PEG (0–33 wt%) and the phosphate buffer (0 – 17 wt%) were tested in 96-deep well plates (Fig. 1c). For ATPE phase diagram construction, both phase forming chemicals were used from stock solutions: 60 wt% PEG and 50 wt% phosphate buffer. A total weight of 1.5 g was evaluated for each ATPE mixture tested. Methyl Orange was added to the mixture to constitute 10 wt% (from a 1 mM solution) as MO migrates exclusively to the top phase in two-phase mixtures (Bensch et al., 2007). The mixture was topped up with Milli-Q water to its final volume. This procedure was identically carried out for all three PEG sizes that were investigated. An additional binodal curve was constructed for each PEG size without MO to determine the baseline absorbance.

Seven mixing steps were performed following the construction of the binodal curves as previously described (7 cycles of 400 μL aspiration and dispense) (Bensch et al., 2007), and then the samples were allowed to rest for 1.5 h, and 100 μL were collected from the bottom of each well to register their absorbance at 450 nm. In single-phase mixtures MO was dispersed throughout the solution and provided higher absorbance readings when compared to the baseline absorbance, while in two-phase mixtures the bottom phase remained clear, showing minimal difference between the experimental and baseline readings.

The mixtures were classified as single-phase ($Abs_{450\,nm} > |0.09|$) or two-phase ($Abs_{450\,nm} < |0.09|$) for the determination of the binodal curve for each PEG size based on the highest difference in absorbance observed between the baseline and a mixture containing MO. The boundary between the single-phase and two-phase regions was used to fit a non-linear regression model to determine the binodal curve. The measurements made along the phase interface were pairwise averaged and these calculated values were used to determine the regression coefficients A, B, and C in Eq. 3 (Merchuk et al., 1998):

$$[PEG] = A \times e^{B \times [K_2HPO_4/KH_2PO_4 \quad]^{1/2} - C \times [K_2HPO_4/KH_2PO_4]} \tag{3}$$

where [PEG] and $[K_2HPO_4/KH_2PO_4]$ in the equation denote wt%.

Table 1
Characteristics of liquids used in this work at 25 °C.

	Density (g cm^{-3})	Viscosity (Pa s)
Water	1.000	6.95×10^{-4}
PEG6000 60 wt%	1.086	3.79×10^{-1}
PEG3000 60 wt%	1.098	1.38×10^{-1}
PEG2000 60 wt%	1.098	0.48×10^{-1}

The regression coefficients were determined using SPSS (SPSS version 25 (IBM Corp., USA)). Subsequent analysis comprised of comparison of these binodal curves with those reported in the literature, and a comparison of these curves obtained from optimised experimental protocols with those repeated using non-optimized transfer parameters (default transfer parameters of the LHD, namely those suitable for water and water-like aqueous solutions). MAE was used as the performance comparison metric.

3. Results and discussion

This work proposes a framework for the identification of the most suitable transfer parameters for automated ATPE. Establishing such a protocol is only possible following a preliminary evaluation of the baseline accuracy and precision of the LHD employed in the study. This is followed by the determination of a series of relationships between the experimental parameters leading to the construction of regression equations, which would then be used to determine the optimal transfer speed, delay time, volume to be transferred, and viscosity (associated with the PEG size and concentration) while minimizing the transfer error. It is important to highlight that the LHD used in this work is able to handle several frequently deployed liquids with different rheological properties through templates built-in to this software. While these templates are practical the fluids they are intended to be used for, such a library would need an extensive corroboration to ensure that the variations in the rheological properties of all possible available mixtures are accounted for, which would be impractical. For this reason, we present an approach below, which can effectively determine the LDH settings for any rheological configuration of interest for liquids employed in a wide range of applications, including but not limited to ATPE. We further utilise this data to develop mathematical equations that successfully relate all the studied parameters to one another for effective transfer of the liquid, which could also account for settings that have not been empirically tested through the models' interpolative predictions.

Finally, in this study, the framework was used to construct the binodal curves for each of the PEGs investigated here and the results obtained from the automated platform were evaluated in conjunction with existing literature. Some relevant properties of the liquids employed here (i.e., viscosity and density) are presented in Table 1. Altogether, these results provide a clear pipeline for the implementation of LHD-driven strategies for handling difficult-to-manipulate liquids or ATPE curve construction.

3.1. Determination of baseline accuracy and precision of water and PEG transfer by LHD

Accuracy and precision are critical parameters that, if not properly determined, will hinder the development of an appropriate experimentation pipeline that is able to deliver correct measurements. Typically, during manual work certain strategies can be applied to compensate for the pipetting errors in liquid transfer when the experimenter is aware of certain challenges associated with the liquids or solutions, such as high viscosity, or surface tension variabilities.

For example, if a liquid is highly viscous, applying the same speed for liquid manipulation as with other non-viscous liquids such as water will produce differences between the expected volume to be transferred and the actual volume displaced. It has been reported that not allowing sufficient interaction time for the displacement caused by pressure difference to act upon highly viscous fluids liquid may cause air cushions to form within the pipetting channel and to be expelled before the liquid gets displaced, thus providing less dispensed liquid (Soh et al., 2023). Observing this phenomenon, an experimenter may adjust their manual pipetting speed as per the requirement of the fluid at hand. While this manually driven on-the-go adjustment may not always allow a high level of accuracy, it may allow experimentation with acceptable variation provided that the experimenter is meticulous and relatively consistent in their practices. The fact that the pipetting tips are typically made of a clear material renders this adjustment possible since visual inspection would be allowed.

This is very different from the case of an LHD, which typically uses black carbon coated DiTis, where visual detection of liquid levels is virtually impossible. Consequently, residual liquid or solution remaining inside the DiTi cannot be removed by corrective actions once a protocol is initiated and running. For this reason, it is critical that all appropriate parameters are configured at their optimum levels prior to execution of any protocol. In order to prevent over-transfer, the device employed in this work was allowed to detect and track liquid level prior to and during aspiration. This allowed the DiTis not to be submerged deep into the reservoir trough and consequently minimise the drag of any liquid on the exterior of a tip. Level detection and tracking are inherent features of the LHD employed in the study. The device utilised carbon-coated tips that are capable of measuring conductivity when submerged in a liquid. Once a tip encounters a change in conductivity such as one that would be induced by the change of ambient from air to a liquid, the robotic arm can halt further immersion and keep the tip at the surface of the liquid or at any requested distance into the liquid. Making use of this feature, the LHD was programmed to aspirate and dispense at the surface of the liquid in order to avoid the exterior of a tip to be dragged with a viscous liquid, which could cause over-transfer or spillage.

As a preliminary evaluation of the baseline viscous liquid transfer performance of the LHD used here, transfers were performed using both the liquid with the highest viscosity employed in this work (PEG6000 60 wt%) and Milli-Q water. The actual mass transferred when 400 μL of either fluid was transferred was recorded. Accurate measurement of mass transfer is very important in the context of ATPE since the construction of binodal curves heavily depend on mass percentages. In order to estimate the accuracy of liquid transfers, the error percentage was recorded for both water and PEG6000 solution and the results were compared. The LHD is very accurate in transferring water when the default liquid transfer parameters were employed, in some cases, with virtually no error (Fig. 2a). In contrast, transfer of PEG6000 yielded errors of up to 10% in all pipette channels, with 17% variability in error. The Mean Absolute Error for PEG6000 was substantially higher than for water, which was within the range reported by the LHD manufacturers, across all pipetting channels (4.82% and 0.94%, respectively) and this difference was significant (p-value < 0.01).

Precision was evaluated by comparing the coefficients of variation (CVs) between the pipetting channels (Fig. 2b). The CV for PEG6000 (0.027) was almost twice as high as that of water (0.015), which was used as the benchmark for the LHD. Variation was detected in all instances of transferring a viscous polymer solution, whereas this was very low, and in some instances virtually zero for transferring water. This highlights the critical necessity to identify appropriate transfer parameters for viscous solutions before venturing into complex and demanding scenarios were multiple volumes and polymers need to be transferred to determine the binodal curves for ATPE.

3.2. Identification of optimal transfer parameters for viscous solutions

In order to identify the optimal transfer parameters for the LDH to be used in subsequent preparation of ATPE mixtures, it is essential to understand the relationship between transfer speed, delay time after transfer, PEG size (or its respective viscosity in a solution), and volume

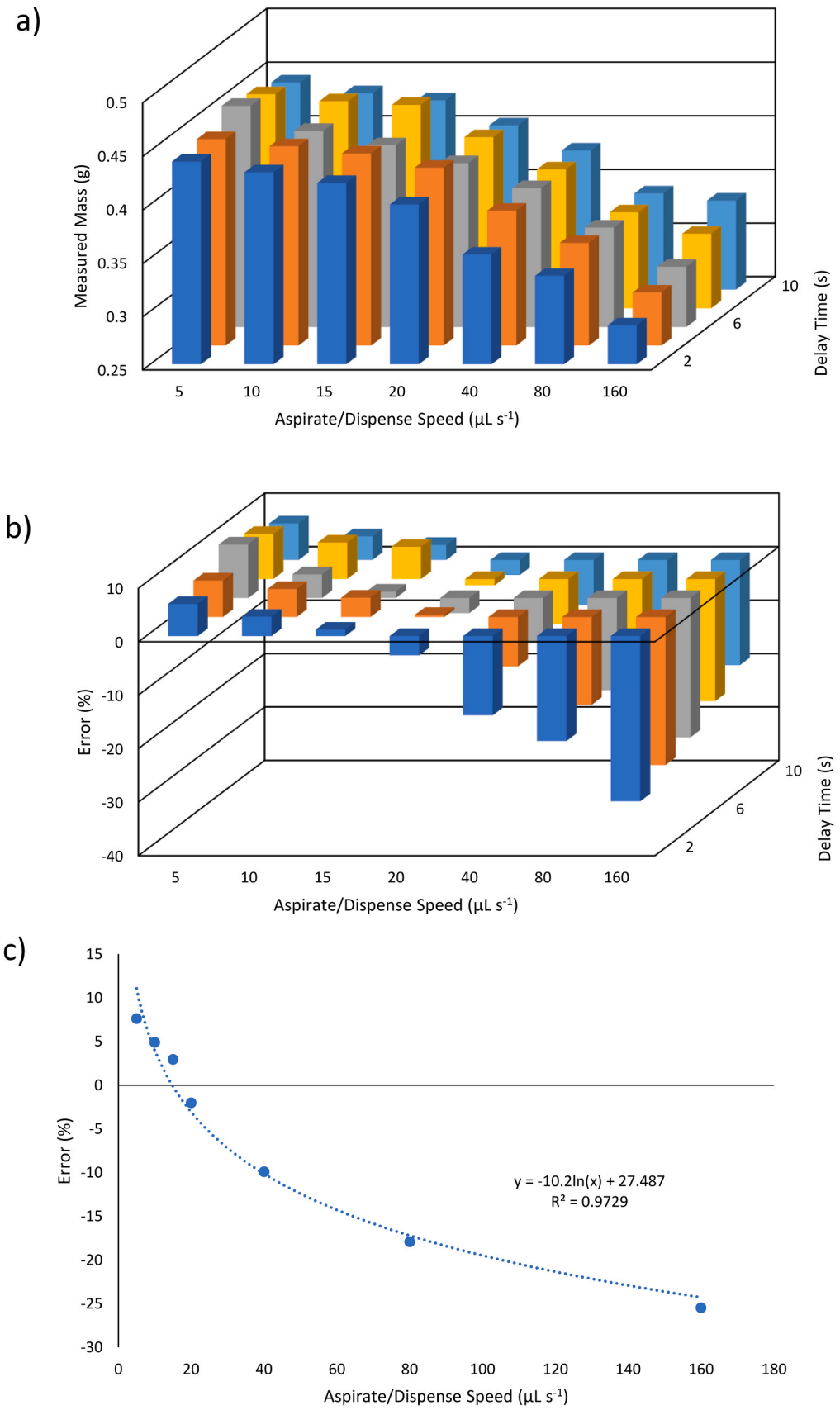

Fig. 3. Effect of aspiration/dispense speed (5–160 µL s^{-1}) and delay time (2–10 s) on the transfer of PEG6000 (60 wt% dispensed at a volume of 400 µL). Results show the relationship between mass transfer, speed and the delay time (a), the error percentage (b), and the relationship between error and fluid transfer speed at a fixed delay time of 10 s (c).

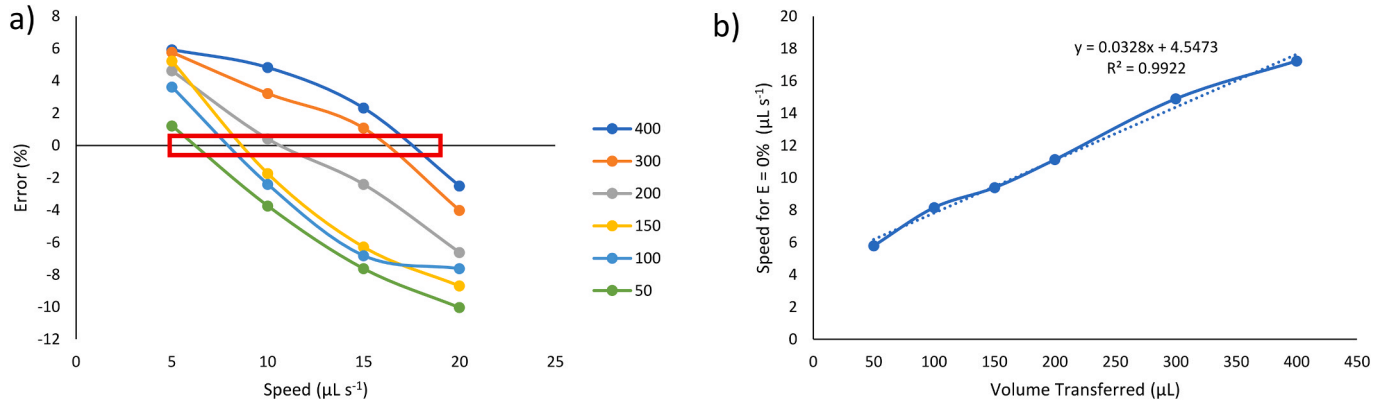

Fig. 4. Effect of aspiration/dispense speed (5–160 µL s^{-1}) and volume (50–400 µL) on the transfer of PEG6000 60 wt%. (a) Results indicate that at the x-intercept, the error will be minimized (0%). This region is indicated by a red box. (b) shows the correlation between specific transfer speeds leading to 0% theoretical error identified for each volume investigated to get a generalisable relationship to determine the optimum transfer speed for any volume of PEG6000 to be transferred.

Table 2
Linear regressions that describe the behavior of aspiration/dispense speed for each volume tested against the percentage of error. The speed for which a minimal error (E = 0%) is expected is included.

Volume (µL)	Slope	Intercept	R^2	Speed for Error = 0%
400	-0.556	9.588	-0.958	17.238
300	-0.629	9.371	-0.978	14.893
200	-0.731	8.133	-0.997	11.126
150	-0.926	8.701	-0.977	9.393
100	-0.763	6.225	-0.955	8.158
50	-0.752	4.349	-0.989	5.782

to be transferred. The first approach used here evaluated the impact of transfer speed and delay time against error percentage after transferring 400 µL of 60%wt PEG6000 (Fig. 3a). Both parameters yielded a statistically significant effect on the actual volume or mass of PEG6000 transferred; the mass transferred was observed to decrease as the transfer speed was increased (p-value < 0.01). This is expected since a viscous liquid would be inclined to resist flow. High transfer speeds allow limited time for the fluid flow, thus resulting in limited amount of fluid to be moved. Following from this notion, a specific transfer speed that will provide a theoretical zero-error percentage can be calculated (Fig. 3b) by setting the error in dispensing/aspirating speed to zero at a fixed delay time of 10 s in a model representing the relationship between the transfer error and transfer speed (Fig. 3c). The delay time following

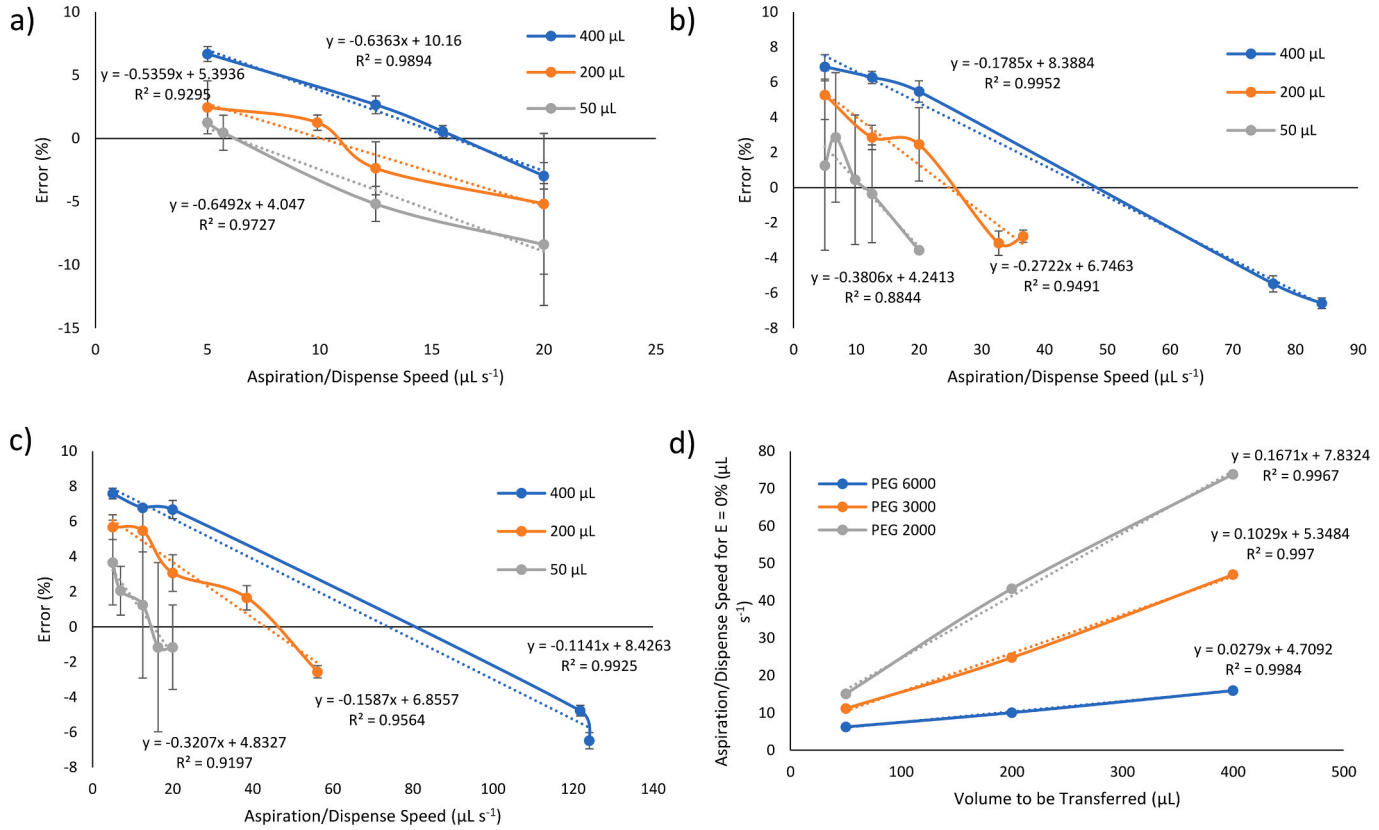

Fig. 5. Effect of aspiration/dispense speed (5–160 µL s^{-1}) and volume (50–400 µL) on the transfer of PEG6000 (a), PEG3000 (b), and PEG2000 (c). Using each regression equation, a transfer speed (for E = 0%) was calculated for each volume and plotted and the regression equations were displayed for each PEG (d).

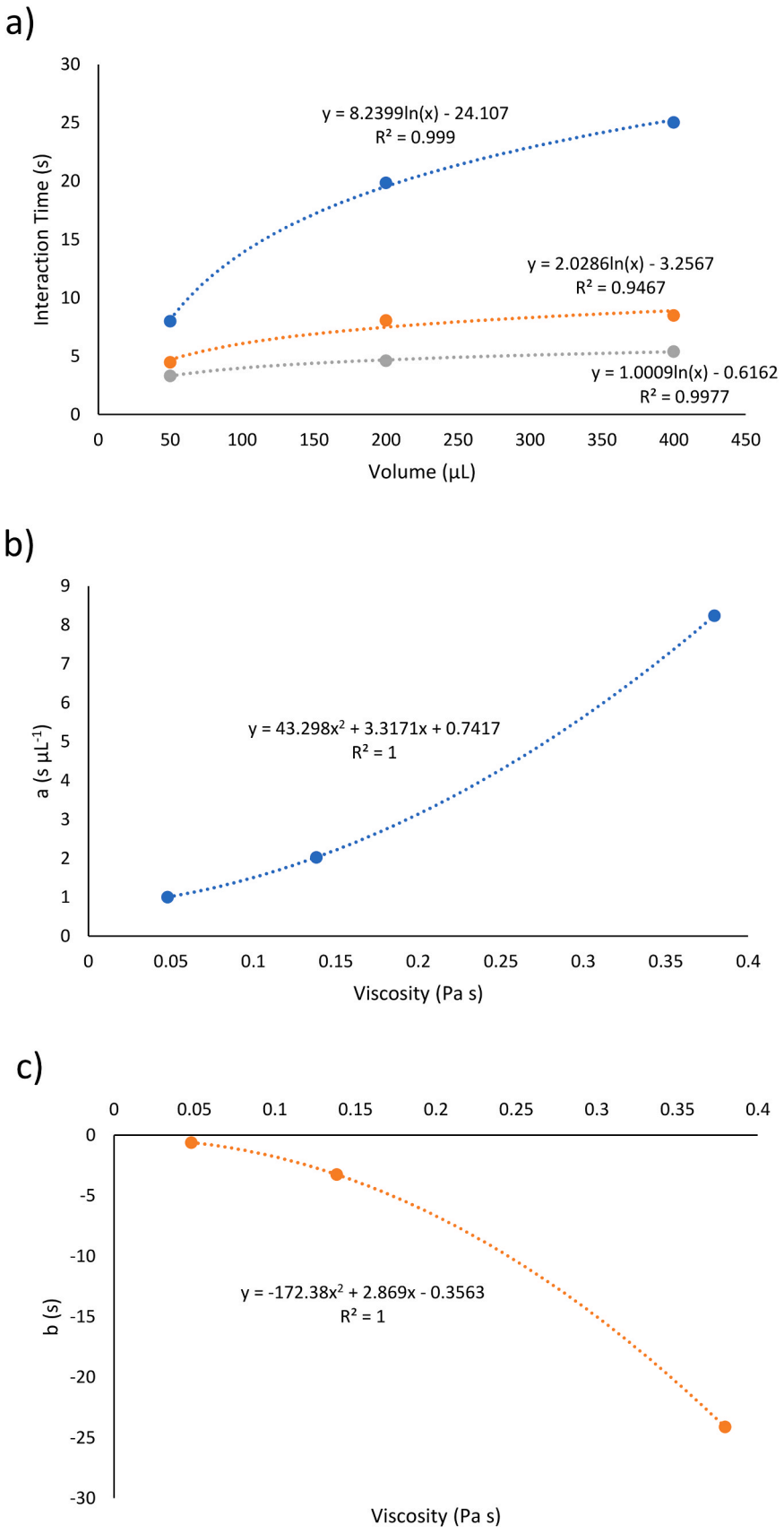

Fig. 6. Relationship of interaction time with volume (a) and viscosity (b and c). The relationships shown in (a) have the form of $y = a \times \ln(x) + b$, where y is interaction time (s) and x is volume to be transferred (µL). Coefficients a and b can be obtained from the relationships shown in (a) and (b) and provide the influence of the viscosity of the solution into the optimal transfer parameters.

the transfer of fluid did not provide a statistically significant effect at speeds below 20 μL s^{-1}, therefore a decision was made to use 10 s delay time as stated earlier (p-value > 0.01). On the other hand, delay time was identified as a critical parameter at high speeds, which allowed the fluid to move along the DiTi following the displacement action.

While in practice it would not be possible to run an experiment maintaining the value of a transfer parameter that should yield an error equal to zero, the calculation of a theoretical value that minimises the error down to 0% is possible. Using this notion, we then evaluated whether there would be a specific speed that provided a theoretical zero-error percentage for each different transfer volume. Considering that delay time did not provide a significant contribution to output variance at speeds below 20 μL s^{-1}, this parameter was fixed at 10 s as before (p-value < 0.01). Transfer speed (5–20 μL s^{-1}) and dispensing volume (50–400 μL) were varied, and the results were compared with the respective mass that was expected to be transferred in order to calculate the error percentages (Fig. 4a). The results showed that the error could indeed be minimized and, theoretically, achieve a zero percentage. The transfer speed must be increased as the volume to be transferred decreased in order to ensure that the error was minimised. The error percentage was shown to display a linear relationship against the volume that was displaced, allowing a regression analysis to be carried out and for theoretical transfer speeds leading to zero error to be calculated (Table 2). The relationship between the calculated theoretical speeds and their cognate transfer volume values yielded to a generalisable relationship that could be used to estimate the most suitable speed for any given volume when PEG6000 was employed (Fig. 4b).

One of the primary goals of carrying out this evaluation was to streamline the automated protocols for constructing the phase diagrams for different compounds, namely in this case, for different PEG sizes leading to varying viscosities. Consequently, the concluding experiment of the preliminary analysis aimed to determine how the speed for appropriate liquid transfer would be affected by PEG size (PEG2000, PEG3000, and PEG6000 in this instance), which leads to change in their viscosity.

As the initial step, the viscosity of each PEG was determined experimentally for stock solutions prepared at 60 wt%. This was followed by an evaluation of whether the speed range determined previously would still be valid for the less viscous samples that will be introduced through PEG2000 and PEG3000. Following this preliminary evaluation (data not shown), a wider range (5–160 μL s^{-1}) of speed was adopted accommodate this variation in viscosity in the following experiments. The speed at which the system can operate with minimal error was determined to increase at low molecular weight, i.e., short polymer length of PEG (Fig. 5a-cfor PEG6000, PEG3000, and PEG2000, respectively). The correlation between the aspiration/dispense speed and the volume of PEG that needed to be displaced in order to obtain a theoretical error equal to zero was determined for fluids with varying viscosities and the cognate correlations were also mathematically represented (Fig. 5d).

Understanding and quantifying the aspiration/dispense speed of DiTi required for displacing different volumes at different viscosities helps to build a universal mathematical relationship that brings this information into a general form will. This, in practice, provides the highest utility from a practical point to facilitate any future ATPE work using PEG solutions, which will aim to utilise an LHD. To address this question, we proposed the following model-driven approach. The variable that differentiated the PEG solutions utilised in this study was viscosity. Solution viscosity and the volume dispensed were modelled using multiple non-linear regression to determine a relationship between these parameters and the fluid transfer speed. In order to address this problem, transfer speed was initially transformed into interaction time (Eq. 4), which is defined as the total time required to transfer a fixed volume and the delay time required for that transfer, which was fixed at 10 s for these experiments. This provided a single value for the two transfer parameters, which represented the overall time that a DiTi was in contact with the liquid to be transferred, which is a relevant variable that is responsible for allowing sufficient time for a sample to enter and exit the DiTi.

$$Interaction\quad Time\quad [s] = \frac{volume\quad to\quad be\quad transferred\quad [\mu L]}{speed\quad for\quad transfer\quad [\mu L\quad s^{-1}]} + Delay\quad time[s] \tag{4}$$

The transfer speeds that yield minimal error for three different volumes of fluid to be transferred (50, 200, and 400 μL) (from Fig. 5**d**) were converted into the newly defined parameter: the interaction time. This parameter was then plotted against the volume of fluid to be transferred (Fig. 6a). This relationship was represented with the mathematical association of the form:

$$Interaction\quad Time\quad [s] = a \times \ln(volume\quad [\mu L]) + b \tag{5}$$

where the coefficients *a* and *b* are determined by their relevant non-linear relationship against viscosity (Fig. 6**b and c**, respectively) and this relationship is mathematically represented by Eqs. 6 and 7, respectively:

$$a = 43.298 \times (viscosity\quad [Pa\quad s])^2 + 3.317 \times (viscosity\quad [Pa\quad s]) + 0.7417 \tag{6}$$

$$b = -47.395 \times (viscosity\quad [Pa\quad s])^2 - 20.42 \times (viscosity\quad [Pa\quad s]) + 10.474 \tag{7}$$

These relationships allowed the estimation of the interaction time, hence the transfer speed required for displacing any volume of fluid at a viscosity that remained within the tested range that would yield the minimum experimental error. The associations developed here clearly demonstrate that the optimisation of operating parameters would allow LHDs to become powerful tools for the deployment of ATPE. The understanding of what the critical variables are and how they behave, together with establishing an optimal setting at which to operate can facilitate and expedite developments for bioprocessing. This has the potential to improve high-throughput screening methodologies to identify the best partitioning and recovery conditions of bioproducts. Using the set of equations developed in this section, it will be possible to explore any ATPE composition considered for the given PEGs studied here. This will be expedited by the construction of the cognate phase diagrams and the identification of the binodal curves.

To determine if this methodology generated a superior manipulation of liquids by modifying transfer parameters, the MAE and CV were recalculated considering optimised parameters. For PEG6000 this resulted in an improvement from 4.82% to 0.75% for the MAE and from 0.027 to 0.008 for the CV. This confirmed that the application of the methodology developed here could indeed reduce variation when transferring viscous liquids. Considering this, it was decided to proceed to the next stage of this research, the determination of binodal curves. The mathematical relationships established here provide a streamlined alternative, a shorthand summary, to identify the full extent of preliminary analysis and optimisation that is required to be executed prior to the implementation of the automation protocol implementing automation. The use of formal or empirical mathematical relationships such as these shown above will ultimately reduce the resources required for optimisation and also aim for minimal introduction of error to achieve cost- and resource-effective experimentation.

3.3. Construction of phase diagrams and binodal curves

Construction of phase diagrams and the corresponding identification of binodal curves within them allows for rational experimentation when using ATPE for product partitioning. Without these, it is not possible to pinpoint ATPE compositions that will be guaranteed to form two phases. The construction of these can be based on different protocols trying to minimize human effort as their manual preparation is labour intensive

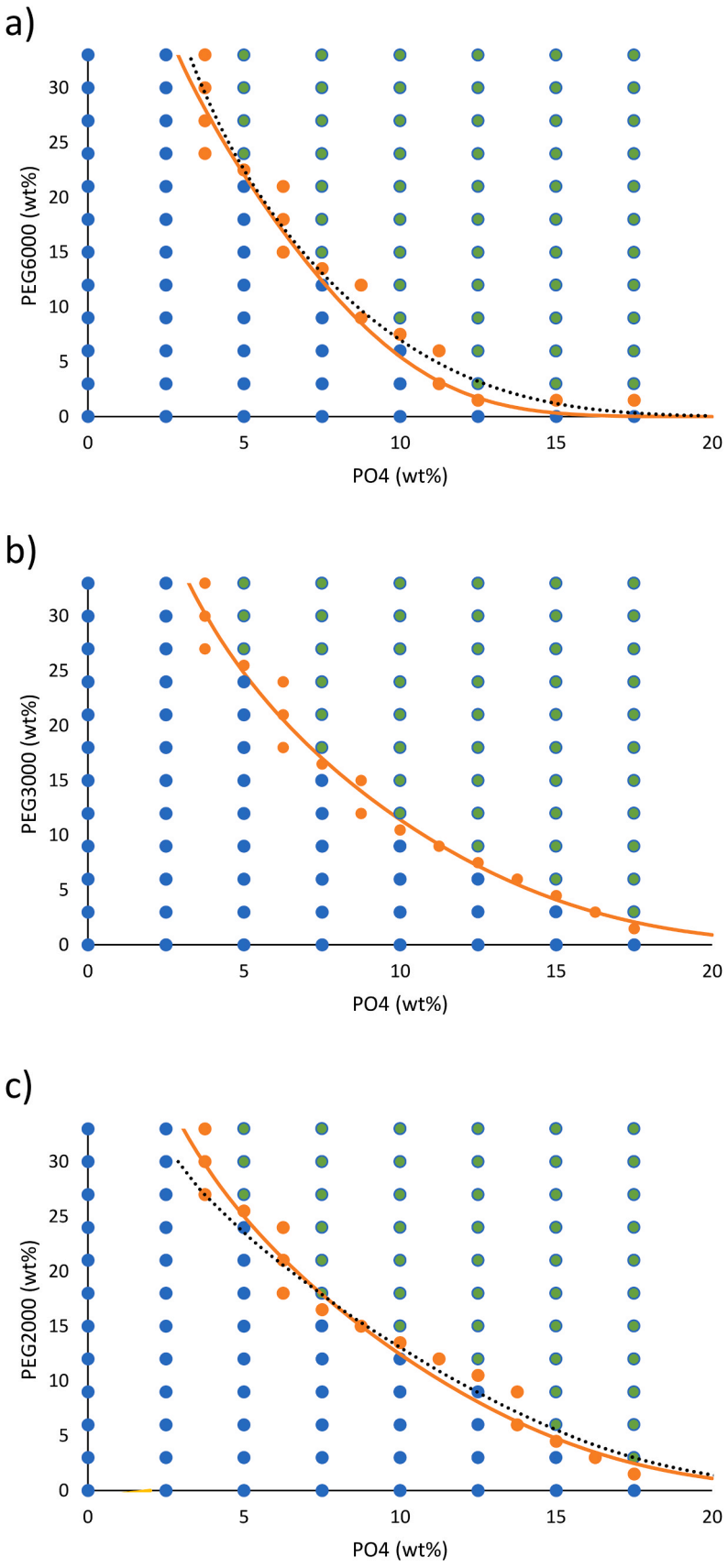

Fig. 7. Phase diagrams for PEG6000 (a), PEG3000 (b), and PEG2000 (c). Each plot contains a binodal curve in orange lines. Black dash lines depict the binodal curves reported in the literature. Orange filled circles indicate the data used for binodal curve construction, which were obtained by averaging the two adjacent points from the one- (blue filled circles) and two-phase regions (green filled circles).

and prone to error. Moreover, for accurate experimentation, a binodal curve with minimal inherent variation must be identified. LHD are useful tools to assist this process of standardising the procedure while fulfilling the criteria for high quality and low variability experimentation. By using an LHD, a wide research space can be explored by testing several ATPE compositions, which would lead to the identification of different volumes (or the corresponding mass of compound) to be transferred during extraction. The accuracy of the phase diagrams will depend entirely on the determination of the optimal transfer parameters as well as the consistent application to minimise variation across runs, thus highlighting the significance of the analyses presented in earlier sections.

In this work, a phase diagram was constructed and the binodal curve was identified using a range of PEG and phosphate compositions (0 – 33 wt% and 0 – 17 wt%, respectively). The relationships presented in Eqs. 4–7 were used to determine the optimal transfer speed at any volume of solution at a given concentration and viscosity of each PEG at 60 wt% to ensure minimal error. The phase diagrams obtained using the non-optimised (default) parameters of the LHD, which are known to be suitable only for water and water-like fluids, did not agree well with the literature. The appropriate selection of operational parameters for handling fluids with varying physiochemical properties allowed the successful identification of the zones for one- and two-phase mixtures (Fig. 7). These binodal curves displayed less steep behaviour for the PEG and phosphate concentrations required to form two phases as PEG size decreased, in line with their expected behaviour. The binodal curves for PEG2000 (Bussamra et al., 2019), constructed using an LHD, and PEG6000 (Fakhari and Rahimpour, 2020), manually constructed, which are available in the literature, were overlain on the results obtained in this experiment for evaluation. A systematic comparison of the binodal curves obtained using optimised settings in this study with those available in the literature yielded MAE of 1.68% and 4.07% for PEG2000 and PEG6000, respectively. The MAE values were determined as 5.97% and 7.38% when the literature values were compared with those obtained using non-optimised liquid transfer parameters in the device for PEG2000 and PEG6000, respectively, demonstrating the clear improvement observed upon the utilisation of optimised parameters. For PEG6000, much of the variation resulted from the value of phosphate recovered at the 0% data point. Removal of that data point reduced the MAE from 7.38% to 4.25% when the default setting of the LHD was utilised, and from 4.07% to 1.79% when the optimised liquid transfer settings were employed. The MAE of 1.68% and 1.79% remained within a 7% error margin, demonstrating that once the viscosity of the fluid was accommodated for in the design of the experiment. These results indicated that the binodal curves constructed in this study using optimised LHD operating parameters were in excellent agreement with the literature, and it was shown that the utilisation of automated platforms specifically yielded very little inter-experiment or inter-laboratory variation highlighting the essential role of utilising automated platforms to streamline this operation.

By performing a precise study of transfer parameters, it was possible to obtain high quality binodal curves that can be employed in future studies. Furthermore, the LHD employed in this study is now equipped with the relevant liquid transfer parameters for efficient experimentation for ATPE. A critical aspect of this process of constructing binodal curves is the use of a relatively limited number of data points. This work employed 96 mixtures in a wide range of concentrations and obtained similar results to the reports available in the literature. Previously, binodal curves were reported to be constructed using an LHD by creating 343 mixtures within a limited range of concentrations (Bussamra et al., 2019). The manual construction of the binodal curve employed approximately 25 mixtures, and the cloud point method, which relies on visual formation of phases, was utilised with the researcher performing the experiments (Fakhari and Rahimpour, 2020). The proposed protocol is sufficiently efficient to allow finetuning of the experimental ranges following a preliminary analysis if high precision is required for the construction of the binodal curves.

4. Conclusions

Currently, there is a lack of a widespread adoption of automation into ATPE. This work serves as a framework to improve and facilitate its inclusion for improving ATPE process development to encourage wider adoption of aqueous two-phase extraction in bioprocessing. Results obtained here highlight the importance of understanding the physicochemical properties of the fluids that are being used and their impact on devices that are typically programmed to work with water or water-like solutions. A systematic deployment of ATPE into a pipeline that utilises LHDs can expedite high-throughput screenings to identify new compositions, ideal conditions for product partition, and assist the optimal use of available resources. Ultimately, all efforts in high-throughput process development at small scale will assist the widespread incorporation of ATPE in large-scale bioprocessing as a low resource-requiring and sustainable alternative for integrated separation of molecules from the fermentation broth. Moreover, this work highlights the complexity of the decisions that have to be made to ensure successful implementation of automation when working with less conventional systems. In this domain of ATPE, the considerations presented here can serve as a guide for researchers and application scientists working with systems that carry similar concerns, and act as a substantial step towards reduction of experimental burden and streamlining of resource allocation while keeping experimental variation and blunders at bay.

Results obtained here demonstrated the need for careful planning and experimental design when incorporating and deploying novel applications into an LHD, with a necessity to optimise operating parameters as and when needed. The lack of accuracy and precision may result in high variability, of up to 17% as observed in this study, and consequently, errors to be introduced to the experimental analysis. The optimisation of the experimental protocols as shown in this work provide relative ease to obtain the specific transfer parameters that yield minimal error in experimentation. This work developed mathematical relationships that show the dependency of the volume to be transferred by the LHD on the viscosity of the fluid to be transferred and the speed at which the process must be carried out. This understanding allowed tailored transfer parameters, which yield minimal error, to be determined and this translated into successful execution of the experiment. Using this framework, similar workflows can be adopted for a wide range of systems with relative ease, which would expand the user-base for automated liquid handling platforms in a variety of different operations.

CRediT authorship contribution statement

Markus Gershater: Validation, Software, Methodology. **Nuno Leitão:** Writing – review & editing, Validation, Software, Methodology. **Gary Lye:** Writing – review & editing, Supervision, Funding acquisition, Conceptualization. **Brenda Parker:** Writing – review & editing, Methodology, Funding acquisition, Formal analysis, Data curation. **Mario Torres-Acosta:** Writing – original draft, Visualization, Methodology, Investigation, Formal analysis, Data curation, Conceptualization. **Ross Kent:** Writing – review & editing, Software, Methodology, Investigation. **Alex Olivares-Molina:** Methodology, Formal analysis, Data curation. **Duygu Dikicioglu:** Writing – review & editing, Supervision, Project administration, Conceptualization.

Declaration of Competing Interest

The authors declare that they have no known competing financial interests or personal relationships that could have appeared to influence the work reported in this paper.

Data Availability

Data will be made available on request.

Acknowledgments

Authors acknowledge funding from University College London's Sustainable Physical and Digital Places for Education and Research (SPiDER) group and support from EPSRC CDT Bioprocess Engineering Leadership (Grant Number EP/L01520X/1). For the purposes of open access, the authors have applied a Creative Commons Attribution (CC BY) licence to any Author Accepted Manuscript version.

Appendix A. Supporting information

Supplementary data associated with this article can be found in the online version at doi:10.1016/j.jbiotec.2024.03.013.

References

Basu, I., Nagappan, R., Fox-Lewis, S., Muttaiyah, S., McAuliffe, G., 2021. Evaluation of extraction and amplification assays for the detection of SARS-CoV-2 at Auckland Hospital laboratory during the COVID-19 outbreak in New Zealand. J. Virol. Methods 289, 114042. https://doi.org/10.1016/j.jviromet.2020.114042.

Bensch, M., Selbach, B., Hubbuch, J., 2007. High throughput screening techniques in downstream processing: preparation, characterization and optimization of aqueous two-phase systems. Chem. Eng. Sci. 62, 2011–2021. https://doi.org/10.1016/j.ces.2006.12.053.

Bessemans, L., Jully, V., de Raikem, C., Albanese, M., Moniotte, N., Silversmet, P., Lemoine, D., 2016. Automated gravimetric calibration to optimize the accuracy and precision of TECAN freedom EVO liquid handler. J. Lab. Autom. 21, 693–705. https://doi.org/10.1177/2211068216632349.

Bussamra, B.C., Gomes, J.C., Freitas, S., Mussatto, S.I., da Costa, A.C., van der Wielen, L., Ottens, M., 2019. A robotic platform to screen aqueous two-phase systems for overcoming inhibition in enzymatic reactions. Bioresour. Technol. 280, 37–50. https://doi.org/10.1016/j.biortech.2019.01.136.

Cibelli, N., Arias, G., Figur, M., Khayat, S.S., Leach, K., Loukinov, I., Shadrick, W., Chuenchor, W., Tsybovsky, Y., Vaccine Production Program Analytical, D., Gulla, K., Gowetski, D.B., 2022. Advances in purification of SARS-CoV-2 spike ectodomain protein using high-throughput screening and non-affinity methods, 4458-4458 Sci. Rep. 12. https://doi.org/10.1038/s41598-022-07485-w.

Cortez, Fd.J., Gebhart, D., Tandel, D., Robinson, P.V., Seftel, D., Wilson, D.M., Maahs, D. M., Buckingham, B.A., Miller, K.W.P., Tsai, C.-t, 2022. Automation of a multiplex agglutination-PCR (ADAP) type 1 diabetes (T1D) assay for the rapid analysis of islet autoantibodies. SLAS Technol. 27, 26–31. https://doi.org/10.1016/j.slast.2021.10.001.

Crone, M.A., Priestman, M., Ciechonska, M., Jensen, K., Sharp, D.J., Anand, A., Randell, P., Storch, M., Freemont, P.S., 2020. A role for biofoundries in rapid development and validation of automated SARS-CoV-2 clinical diagnostics, 4464-4464 Nat. Commun. 11. https://doi.org/10.1038/s41467-020-18130-3.

Czernek, K., Witczak, S., 2020. Precise determination of liquid layer thickness with downward annular two-phase gas-very viscous liquid flow. Energies 13. https://doi.org/10.3390/en13246529.

Fakhari, M.A., Rahimpour, F., 2020. Measurements and thermodynamic modelling of liquid–liquid equilibrium of PEG 6000–phosphate affinity aqueous two-phase systems at various ligand concentrations and pH. Phys. Chem. Liq. 58, 483–499. https://doi.org/10.1080/00319104.2019.1611824.

Groth, P., Cox, J., 2017. Indicators for the use of robotic labs in basic biomedical research: a literature analysis. e3997-e3997 PeerJ 5. https://doi.org/10.7717/peerj.3997.

Iqbal, M., Tao, Y., Xie, S., Zhu, Y., Chen, D., Wang, X., Huang, L., Peng, D., Sattar, A., Shabbir, M.A.B., Hussain, H.I., Ahmed, S., Yuan, Z., 2016. Aqueous two-phase system (ATPS): an overview and advances in its applications. Biol. Proced. Online 18, 18. https://doi.org/10.1186/s12575-016-0048-8.

Kiesewetter, A., Menstell, P., Peeck, L.H., Stein, A., 2016. Development of pseudo-linear gradient elution for high-throughput resin selectivity screening in RoboColumn® Format. Biotechnol. Prog. 32, 1503–1519. https://doi.org/10.1002/btpr.2363.

Kojima, T., Lin, C.-C., Takayama, S., Fan, S.-K., 2019. Determination of aqueous two-phase system binodals and tie-lines by electrowetting-on-dielectric droplet manipulation. ChemBioChem 20, 270–275. https://doi.org/10.1002/cbic.201800553.

Kruse, T., Kampmann, M., Rüddel, I., Greller, G., 2020. An alternative downstream process based on aqueous two-phase extraction for the purification of monoclonal antibodies. Biochem. Eng. J. 161, 107703 https://doi.org/10.1016/j.bej.2020.107703.

Mao, L.N., Rogers, J.K., Westoby, M., Conley, L., Pieracci, J., 2010. Downstream antibody purification using aqueous two-phase extraction. Biotechnol. Prog. 26, 1662–1670. https://doi.org/10.1002/btpr.477.

Merchuk, J.C., Andrews, B.A., Asenjo, J.A., 1998. Aqueous two-phase systems for protein separation: studies on phase inversion. J. Chromatogr. B Biomed. Sci. Appl. 711, 285–293. https://doi.org/10.1016/S0378-4347(97)00594-X.

Paton, T.F., Marr, I., O'Keefe, Z., Inglis, T.J.J., 2021. Development, deployment and in-field demonstration of mobile coronavirus SARS-CoV-2 nucleic acid amplification test. J. Med. Microbiol. 70, 001346 https://doi.org/10.1099/jmm.0.001346.

Rahbari-Sisakht, M., Taghizadeh, M., Eliassi, A., 2003. Densities and viscosities of binary mixtures of poly(ethylene glycol) and poly(propylene glycol) in water and ethanol in the 293.15−338.15 K temperature range. J. Chem. Eng. Data 48, 1221–1224. https://doi.org/10.1021/je0301388.

Rosa, P.A.J., Azevedo, A.M., Sommerfeld, S., Mutter, M., Aires-Barros, M.R., Bäcker, W., 2009. Application of aqueous two-phase systems to antibody purification: a multi-stage approach. J. Biotechnol. 139, 306–313. https://doi.org/10.1016/j.jbiotec.2009.01.001.

Schmidt, A., Richter, M., Rudolph, F., Strube, J., 2017. Integration of aqueous two-phase extraction as cell harvest and capture operation in the manufacturing process of monoclonal antibodies. Antibodies. https://doi.org/10.3390/antib6040021.

Silva, D.F.C., Azevedo, A.M., Fernandes, P., Chu, V., Conde, J.P., Aires-Barros, M.R., 2014. Determination of aqueous two phase system binodal curves using a microfluidic device. J. Chromatogr. 1370, 115–120. https://doi.org/10.1016/j.chroma.2014.10.035.

Soh, B.W., Chitre, A., Lee, W.Y., Bash, D., Kumar, J.N., Hippalgaonkar, K., 2023. Automated pipetting robot for proxy high-throughput viscometry of Newtonian fluids. Digit. Discov. https://doi.org/10.1039/D2DD00126H.

Taylor, S.C., Hurst, B., Martiszus, I., Hausman, M.S., Sarwat, S., Schapiro, J.M., Rowell, S., Lituev, A., 2021. Semi-quantitative, high throughput analysis of SARS-CoV-2 neutralizing antibodies: measuring the level and duration of immune response antibodies post infection/vaccination. Vaccine 39, 5688–5698. https://doi.org/10.1016/j.vaccine.2021.07.098.

Torres-Acosta, M.A., Mayolo-Deloisa, K., Gonzalez-Valdez, J., Rito-Palomares, M., 2019. Aqueous two-phase systems at large scale: challenges and opportunities. Biotechnol. J. 14, e1800117 https://doi.org/10.1002/biot.201800117.

Torres-Acosta, M.A., Lye, G.J., Dikicioglu, D., 2022. Automated liquid-handling operations for robust, resilient, and efficient bio-based laboratory practices. Biochem. Eng. J. 188, 108713 https://doi.org/10.1016/j.bej.2022.108713.

Tripathi, N.K., Shrivastava, A., 2019. Recent developments in bioprocessing of recombinant proteins: expression hosts and process development. Front. Bioeng. Biotechnol. 7, 420.

Villanueva-Cañas, J.L., Gonzalez-Roca, E., Gastaminza Unanue, A., Titos, E., Martínez Yoldi, M.J., Vergara Gómez, A., Puig-Butillé, J.A., 2021. Implementation of an open-source robotic platform for SARS-CoV-2 testing by real-time RT-PCR. PLoS One 16, e0252509. https://doi.org/10.1371/journal.pone.0252509.

Wang, H., Kelley, F., Milovanovic, D., Schuster, B.S., Zheng, S., 2021. Surface tension and viscosity of protein condensates quantified by micropipette aspiration. Biophys. Rep. 1 https://doi.org/10.1016/j.bpr.2021.100011.